Published in final edited form as:
Arterioscler Thromb Vasc Biol. 2023 February ; 43(2): 323–329. doi:10.1161/ATVBAHA.122.318006.

Differential expression of inflammarafts in macrophage foam cells and in non-foamy macrophages in atherosclerotic lesions

Juliana M. Navia-Pelaez[*],
Colin Agatisa-Boyle[*],
Soo-Ho Choi[*],
Yi Sak Kim,
Shenglin Li,
Elena Alekseeva,
Kimberly Weldy,
Yury I. Miller[#]
Department of Medicine, University of California, San Diego, La Jolla, CA

Abstract

Background: Reprogramming of monocytes and macrophage manifests in hyperinflammatory responses and chronification of inflammation in atherosclerosis. Recent studies focused on epigenetic, transcriptional and metabolic alterations that characterize trained immunity. However, the underlying effector mechanisms driving the hyperinflammatory response of reprogrammed macrophages remain unclear. We hypothesized that the plasma membrane of atherosclerotic lesion macrophages undergoes reprogramming to maintain inflammarafts, enlarged lipid rafts (LR) serving as a platform for assembly of inflammatory receptor complexes.

Methods: Single cell suspensions from the aortae of Western diet-fed *Ldlr*$^{-/-}$ mice were gated for BODIPY-high foamy and BODIPY-low non-foamy F4/80 macrophages by flow cytometry. Inflammarafts were characterized by increased levels of LR, TLR4 localization to LR, TLR4 dimers, and the proximity between TLR2, TLR1 and CD36. In a cellular model of trained immunity, LR, TLR4 dimers and the inflammatory response were measured in bone marrow-derived macrophages (BMDM) subjected to a 24-hour treatment with LPS or OxLDL, followed by a 6-day wash-out period.

Results: Non-foamy macrophages, which constituted approximately 40% of macrophages in atherosclerotic lesions, expressed significantly higher levels of LR and TLR4 dimers, as well as proximity ligation signals for TLR4-LR, TLR2-CD36 and TLR2-TLR1 complexes, compared

[#] Correspondence to Yury I. Miller, yumiller@health.ucsd.edu.
[*]Equal contribution

DISCLOSURES
Y.I.M. is scientific co-founder of Raft Pharmaceuticals LLC. The terms of this arrangement have been reviewed and approved by the University of California, San Diego in accordance with its conflict of interest policies. Other authors declare that they have no competing interests.

SUPPLEMENTAL MATERIAL
Supplemental Figures S1 – S3
Major Resources Table

to foamy macrophages. These inflammaraft measures associated, to a different degree, with plasma cholesterol and inflammatory cytokines, as well as the size of the atherosclerotic lesions and necrotic cores. The BMDM trained with LPS simulated non-foamy atherosclerotic lesion macrophages and continued to express inflammarafts and inflammatory genes for 6 days after LPS removal and displayed a hyperinflammatory response to Pam3CSK4, a TLR2/TLR1 agonist. OxLDL-exposed, lipid-laden macrophages did not express inflammarafts.

Conclusions: Our data support the hypothesis that persistent inflammarafts in non-foamy macrophages in atherosclerotic lesions serve as effectors of macrophage reprogramming into a hyperinflammatory phenotype.

Graphical Abstract

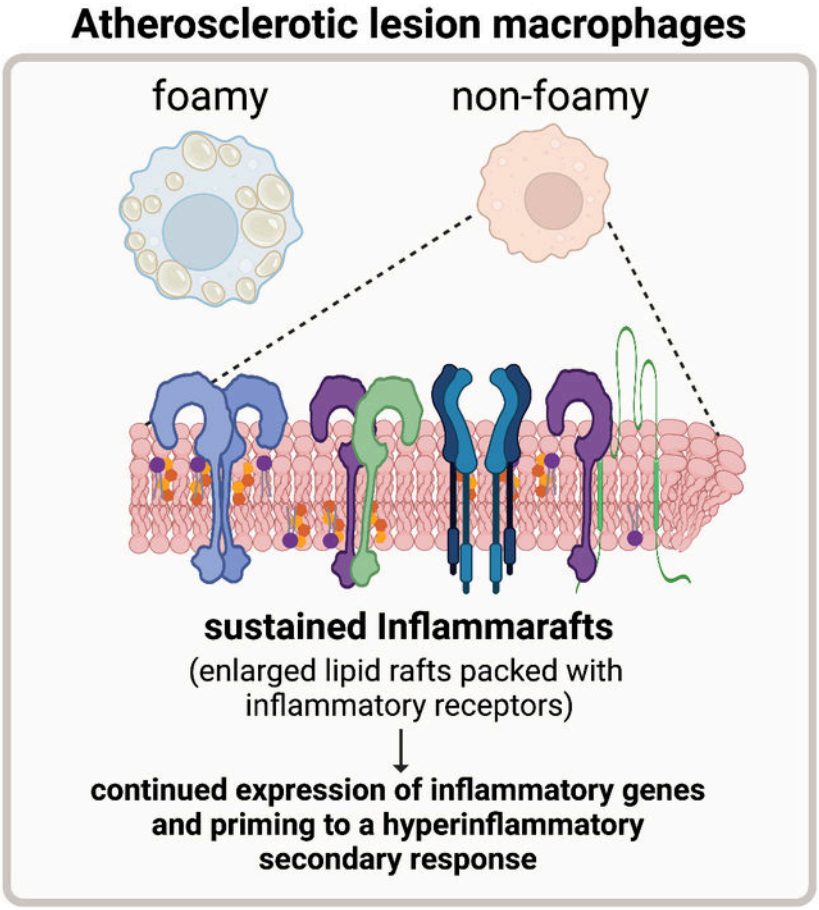

INTRODUCTION

The concept of trained immunity is rapidly gaining acceptance as it helps explain how chronic inflammatory diseases develop [1]. The chronification of inflammation results from the reprogramming of monocytes and macrophages to alter their metabolic, epigenetic, and transcriptional regulation [1–3]. This long-lasting reprogramming manifests in a hyperinflammatory response to the subsequent, secondary insult, which could be bacterial or viral infection, exposure to an allergen, or a seemingly benign condition of post-

prandial, subclinical endotoxemia. Trained immunity also contributes to pathologies with persistent generation of endogenous, damage-associated molecular patterns (DAMPs), such as oxidized lipids associated with hyperlipidemia, which contribute to the development of atherosclerosis. A large number of recent studies of trained immunity focused on histone modification, DNA methylation and the balance between oxidative phosphorylation and glycolysis in immune cells [1–3]. Less attention was given to the underlying mechanisms and the molecular machinery responsible for the hyperinflammatory response of reprogrammed cells.

We hypothesize that the plasma membrane of vascular macrophages in atherosclerosis undergoes reprogramming to maintain inflammarafts. We define inflammarafts as enlarged, cholesterol-rich lipid rafts hosting receptors, enzymes and adaptor molecules assembled for a rapid and augmented inflammatory response [4]. Lipid rafts in quiescent cells are highly dynamic and transient. Upon cell activation, lipid rafts cluster and become more stable to accommodate agonist-induced receptors assembly, e.g., LPS-induced TLR4 dimerization, and initiation of signaling, which within minutes leads to receptor-ligand endocytosis. However, in a study of mechanisms underlying neuropathic pain, we observed TLR4 dimers and enlarged lipid rafts in spinal microglia as late as 3 weeks after a chemotherapeutic intervention, which resulted in peripheral neuropathy [5]. These results suggest microglia reprogramming and persistent maintenance of TLR4 inflammarafts in a chronic inflammatory state.

In the present study, in the context of atherosclerosis, we analyzed inflammarafts in two major macrophage populations found in atherosclerotic lesions: lipid-laden, foamy macrophages and non-foamy macrophages reported to have an inflammatory phenotype [6]. In addition, we used a cellular model of bone marrow-derived macrophages (BMDM) treated with OxLDL and LPS to replicate features of foamy and inflammatory macrophages.

MATERIALS AND METHODS

The authors will make their data, analytic methods, and study materials available to other researchers upon request.

Animals and diet and assessment of atherosclerosis

All experiments were conducted according to protocols approved by the Institutional Animal Care and Use Committee of the University of California, San Diego. *Ldlr*$^{-/-}$ mice were bred in-house and housed up to 4 per standard cage at room temperature and maintained on a 12:12-hour light:dark cycle. Both male and female mice were used for experiments. Starting at 8 weeks of age, *Ldlr*$^{-/-}$ mice were fed for 20 weeks a Western-type, high-fat diet (Envigo TD.88137) containing 0.2% cholesterol and 42% kcal from fat. Upon sacrifice, mice were perfused for 5 minutes using ice cold PBS and the aortae were dissected and prepared for flow cytometry analyses described below. The hearts were embedded in paraffin, and atherosclerosis was assessed as previously described [7]. To quantify aortic root atherosclerosis, 10 sections were cut from the aortic origin to the last leaflet. Sections were stained using a modified Gomori's protocol, and the size of atherosclerotic lesions and of necrotic cores were quantified via computer-assisted image analysis (ImagePro) [7].

Plasma cholesterol was measured using a BioVision's K632-100 kit. Plasma protein levels of MCP-1, TNFα, IL-1β and IL-6 were measured in ELISA using reagents from R&D Systems.

Human tissue samples

Human carotid endarterectomy specimens were obtained from patients undergoing carotid endarterectomy with a protocol approved by the University of California, San Diego Human Research Protection Program.

Aorta single cell suspension

The aortae were cleaned of adipose tissue, cut into several sections and digested for 1 hour at 37°C in HBSS containing 250 U/mL collagenase type XI, 120 U/mL hyaluronidase type 1-s, 120 U/mL DNase I and 450 U/mL collagenase type I. The digested aortae were then passed through a 75 μM cell strainer after which cells were pelleted by centrifuging at 500 g for 5 min and resuspended in RPMI containing 10% FBS. The single cell suspensions were incubated at 37°C for 15 minutes to allow cell surface recovery following enzymatic digestion. Lipid droplets were stained with 1 μg/mL BODIPY at 37°C for 15 minutes. Cells were then fixed using 3.7% formaldehyde for 10 minutes at room temperature.

Flow cytometry analyses of inflammaraft

Aortic cell suspensions were blocked using an anti-CD16/CD32 antibody in buffer containing 2% BSA and 2% mouse serum for 30 minutes on ice. Cells were then incubated for 45 min at 4°C with a mixture of PE-Cy7-conjugated anti-CD45, PerCP Cy5.5-conjugated F4/80, PE-conjugated TLR4/MD2 (MTS510) and APC-conjugated total TLR4 (SA15-21) antibodies, and Alexa Fluor 594-conjugated CTxB, for 45 minutes on ice. After staining, cells were washed and analyzed using a CytoFLEX flow cytometer (Beckman Coulter). To calculate TLR4 dimers, the ratio of the geometric mean fluorescence intensity of PE-conjugated TLR4/MD2 (MTS510) antibody over APC-conjugated total TLR4 (SA15-21) antibody was calculated [5]. Splenic F4/80 positive macrophages obtained from *Ldlr*$^{-/-}$ mice fed a standard laboratory diet and treated for 15 min with LPS (to induce transient TLR4 dimerization) served as a positive control for the TLR4 dimer assay. Non-stimulated splenic macrophages served as a negative control and to standardize data obtained over time.

LDL oxidation

Human native LDL was purchased from Lee Biosolutions (360-10). OxLDL was produced *in vitro* as previously reported [8]. Briefly, LDL was extensively dialyzed against PBS to remove EDTA, and 0.1 mg/mL of LDL was incubated with 10 μM $CuSO_4$ for 18 h at 37°C. Thiobarbituric acid reactive substances (TBARS; typically, more than 30 nmol/mg in OxLDL) were measured to confirm LDL oxidation. OxLDL was concentrated to 1 mg/mL using a 100 kDa cut off centrifugal concentrator (Millipore, UFC810024) and sterile filtered (0.22 μm). Endotoxin contamination was tested using a Pierce Chromogenic Endotoxin Quant Kit (Thermo Fisher, A39553), and only LDL preparations with endotoxin levels below 0.025 EU/mg protein were used in this study.

Bone marrow-derived macrophages

BMDM were cultured as previously described [8]. In brief, bone marrow cells were isolated from femurs and tibias of 8-week-old C57BL/6J male mice and cultivated in L929 conditioned medium. After one week, cells were replated in 6-well plates at a density of 1 million cells per well. Cells were incubated with either vehicle (DMEM supplemented with 5% lipoprotein-deficient serum), 20 μg/mL OxLDL, or 100 ng/mL LPS (Kdo2-LipidA). After 24 hours, cells in half of the plates were harvested by gentle scrapping. Lipid droplets were stained with 1 μg/mL BODIPY in PBS for 15 minutes at 37°C. Following BODIPY staining, cells were fixed with 3.7% formaldehyde for 10 minutes at room temperature. The remaining plates were incubated in L929 conditioned medium containing 10% FBS for six days after which cells were either: 1) stained with BODIPY and fixed as previously described, 2) harvested for RNA isolation, or 3) underwent secondary stimulation for 4 hours with vehicle, Pam3CSK4 (10 ng/mL) or LPS (10 ng/mL).

Isolation of lipid rafts

Lipid rafts were isolated using a detergent-free, discontinuous gradient ultracentrifugation method as in our earlier work [9]. In brief, cells were harvested into 1 mL of 0.5 M sodium bicarbonate buffer (pH 11) containing a protease inhibitor cocktail, homogenized and sonicated. One mL of disrupted cell suspension was mixed with 1 mL of 90% sucrose in MBS (25 mM 2-(N-morpholino)ethanesulfonic acid, pH 6.5, 150 mM NaCl) to adjust to 45% sucrose and placed into ultracentrifugation tubes. Four mL of 5–35% discontinuous sucrose gradient in MBS containing 250 mM sodium bicarbonate was formed above the sample. Following ultracentrifugation at 35,000 rpm in a SW-41 rotor (Beckman) for 20 hours at 4^{o}C, ten 1 mL fractions were collected from top to bottom. The lipid raft fractions 4 and 5 were combined, supplemented with 8 mL of MBS buffer and subjected to an additional round of ultracentrifugation at 35,000 rpm for 2 hours at 4^{o}C. The pellet was resuspended in LDS sample buffer (Invitrogen), and samples were run on a NuPAGE gel, transferred to a PVDF membrane and immunoblotted with the indicated antibodies. Band densities were measured using ImageJ, and TLR4 density was normalized to that of FLOT1 for each sample.

Proximity ligation assay

TLR4-lipid rafts (TLR4-LR), TLR2-CD36, TLR2-TLR1, and IFNγR1-IFNγR2 assemblies were assessed using Duolink PLA reagents from Sigma. Briefly, after incubation with BODIPY, cell suspensions were fixed and incubated with unconjugated CTxB for 30 min and then with probe-conjugated antibodies for 1 hour at 37°C. Ligation was performed for 30 min and amplification overnight at 37°C. After amplification, a detection step was performed, and cells were counterstained with PE-Cy7-conjugated anti-CD45 and PerCP-Cy5.5-conjugated anti-F4/80 antibodies. Following staining, cell suspensions were washed three times with cold PBS, and analyzed using a CytoFLEX flow cytometer. Macrophages (F4/80+ cells) were gated for foamy and non-foamy macrophages based on BODIPY staining and size (FSC). The percentage of PLA positive cells was quantified separately for foamy and non-foamy macrophages in each aorta cell suspension using FlowJo software. The same reagents and protocol were used for PLA of tissue sections,

which were imaged using a Leica SP8 microscope. Regular immunohistochemistry staining with antibodies used for PLA conjugation was used as positive controls for PLA assay and PLA protocol including primary antibodies but excluding amplification reagent for the assay were performed as negative controls.

Quantitative PCR

Total RNA was isolated using Nucleospin RNA columns (Clontech). cDNA was synthesized from isolated RNA using cDNA EcoDry (Clontech), following manufacturer's instruction. Quantitative PCR was performed using a AzuraView GreenFast qPCR Blue Mix LR (Azura Genomics, AZ-2320), with primers ordered from Integrated DNA Technologies (IDT), and a Rotor Gene Q thermocycler (Qiagen). The ΔΔCt method was used for comparisons of mRNA abundance, and *Cyclophilin A* (*CypA*) was used as internal gene control.

Statistical Analyses

Data were represented as Mean±SEM. N represents biological replicates. Data were analyzed for normality and equal variance using Kolmogorov-Smirnov's test. Student's *t* test (2-sided) was used to compare 2-group data; paired *t* test was used for analysis of foamy vs. non-foamy macrophages from the same sample. For multiple-group data with 1 or 2 independent factors, one- or two-way ANOVA with Tukey's or Dunnett's multiple comparison test were applied for normally distributed variables. All statistical analyses were conducted using GraphPad Prism, version 9.4.1. $P<0.05$ was considered as statistical significance.

RESULTS

Characteristics of inflammarafts in atherosclerotic lesion macrophages

Single cell suspensions from the aortae of Western diet-fed $Ldlr^{-/-}$ mice were gated for BODIPY-high foamy and BODIPY-low non-foamy F4/80 macrophages, which were present at a 60:40 ratio (Figure 1A and 1B and Figure S1). The cells were further analyzed for the levels of cholera toxin B (CTxB)-positive lipid rafts and TLR4 dimers, which characterize inflammarafts [5]. F4/80-positive splenocytes from age-matched, standard laboratory diet-fed $Ldlr^{-/-}$ mice, treated for 15 min with vehicle or LPS served as negative and positive controls for inflammarafts. Non-foamy aortic macrophages maintained significantly higher levels of TLR4 dimers and lipid rafts than foamy macrophages, and higher than in the splenocytes acutely stimulated with LPS (Figure 1B). We next used a proximity ligation assay (PLA) to examine whether inflammarafts in atherosclerotic lesion macrophages host other than the TLR4 homodimer receptor assemblies. Practically all non-foamy macrophages in all mice expressed TLR2-CD36 and TLR2-TLR1 complexes, while TLR4 localization to lipid rafts (TLR4-LR) and IFNγR1-IFNγR2 varied between mice. All receptor complexes but the IFNγR pair were significantly higher in non-foamy than foamy macrophages (Figure 1C). The PLA imaging of inflammaraft components in mouse aortic roots supported the flow cytometry findings of higher expression of TLR2-CD36 compared to TLR4-LR (Figure 1D). However, in human carotid artery, TLR4-LR was more abundant than TLR2-CD36 (Figure 1D), indicating potentially different balance of inflammatory mechanisms in human and mouse atherosclerotic lesions.

To examine association of inflammaraft parameters with established inflammatory markers and the extent of atherosclerosis, we measured plasma total cholesterol and cytokine levels and the size of atherosclerotic lesions (Figure 1 E and 1F). TLR4-LR and IFNγR1-IFNγR2 in non-foamy macrophages correlated with MCP-1, IL-1β and IL-6 but not TNFα plasma levels, and TLR2-CD36 correlated with MCP-1 only. There was a significant association between inflammaraft components and total plasma cholesterol but only a trend toward association with the lesion size. The size of necrotic cores correlated only with TLR2-TLR1 but not the other receptor pairs.

Characteristics of inflammarafts in a cellular model of trained immunity

In vitro, a short exposure of splenic macrophages to the TLR4 ligand LPS not only induced TLR4-LR but also TLR2-TLR1 assembly, and conversely, the TLR2/TLR1 ligand Pam3 induced TLR4-LR (Figure 1C), suggesting that one agonist can prime macrophages for a hyperinflammatory response to a different subsequent stimulus. We further explored these possibilities in a cellular model of trained immunity[2].

BMDM were subjected to a 24-hour treatment with LPS or OxLDL, followed by a 6-day wash-out period and then a 4-hour stimulation with Pam3CSK4 (TLR2/TLR1 agonist) or LPS; the cells were analyzed at each of these three time points (Figure 2A). At 24 hours, OxLDL and LPS had the opposite effects on the BMDM phenotype: OxLDL induced accumulation of lipid droplets but reduced overall surface TLR4 expression and TLR4 dimers; the LPS treatment did not induce lipid accumulation but resulted in significant increases of TLR4 dimers and lipid rafts (Figure 2B and Figure S2). Remarkably, the TLR4 inflammaraft phenotype persisted in BMBM for 6 days after LPS removal (Figure 2C). The increased occupancy of TLR4 in lipid rafts of LPS-trained macrophages after the 6-day wash-out was confirmed with western blot analysis of lipid raft fractions obtained by gradient density ultracentrifugation (Figure 2D).

Even after the 6-day wash-out, the LPS-trained BMDM continued to express higher levels of *Cxcl2*, *Il6* and *Il1b* mRNA compared to vehicle, but *Ccl2* and *Tnf* levels were not increased (Figure 2E). Predictably, BMDM treated with 100 ng/ml LPS were tolerant to a second LPS stimulation (Figure S3). However, the LPS-trained cells displayed hyperinflammatory *Cxcl2*, *Il6* and *Il1b* (but not but *Ccl2* or *Tnf*) responses to Pam3 compared to cells exposed to vehicle or OxLDL (Figure 2F). These results support our hypothesis that characteristics of inflammarafts associate with a macrophage trained immunity phenotype.

DISCUSSION

In this study, we demonstrated that macrophages in atherosclerotic lesions and in model cellular systems differentially express inflammarafts – enlarged lipid rafts harboring receptors, which are positioned in close proximity for a rapid and heightened inflammatory response. Non-foamy macrophages possess a higher density of inflammarafts than lipid-laden macrophage foam cells, which agrees with the findings of single cell transcriptomic analyses showing an inflammatory phenotype of non-foamy macrophages [6]. We also identified a number of associations between PLA-detected inflammaraft measures and systemic inflammatory and atherosclerosis burden parameters. The TLR4-LR PLA,

measuring TLR4 localization to lipid rafts, correlated with plasma levels of cholesterol, MCP1, IL-6 and IL-1β. None of the PLA measures correlated with plasma TNFα levels, and in agreement, *Tnf* expression was not increased in LPS-trained BMDM. The size of necrotic core in atherosclerotic lesions correlated only with TLR2-TLR1 but no other PLA pairs. These results and future studies may contribute to a better understanding of the composition of an inflammatory milieu, which governs the development of atherosclerosis.

The mechanisms underlying chronic maintenance of inflammarafts in atherosclerosis remain to be elucidated. They may include reduced cholesterol efflux and other components of metabolic reprogramming including lipidome reprograming [10], persistent generation of DAMPs and metabolic endotoxemia, and reprogramming of the endocytosis process to slow down internalization of inflammatory receptors and/or to accelerate their recycling. Likewise, the exact molecular architecture of inflammarafts needs to be examined by biophysical methods. However, published evidence [11] suggests that in addition to a modest increase in the overall size of lipid rafts in activated cells, as we detected in this work, these rafts tend to cluster to form significantly larger individual rafts. These clustered lipid rafts can accommodate packing in close proximity of a large number of inflammatory receptors poised to a hyperinflammatory response to secondary stimuli. We observed that an exposure of splenic macrophages to the TLR4 ligand LPS induced TLR2-TLR1 assembly, and the TLR2/TLR1 ligand Pam3 increased TLR4 localization to lipid rafts. In addition, LPS-primed BMDM responded to Pam3 with a higher expression of inflammatory cytokines than control cells. These results suggest that one agonist can prime macrophages – via formation of inflammarafts that host a community of inflammatory receptors – for a hyperinflammatory response to a broad spectrum of secondary stimuli. Atherosclerotic lesions flooded with DAMPs and occasionally exposed to microbial pathogens is the fertile ground for maintaining inflammarafts by non-foamy macrophages primed for a rapid and augmented inflammatory signaling.

In contrast to the reported hyperinflammatory responses of human monocytes trained with OxLDL [12], our studies with OxLDL-exposed BMDM did not show any increased response to re-stimulation with LPS or Pam3. This may be due the differences between human monocytes and mouse BMDM and/or to the differences in OxLDL composition, which is notoriously difficult to control, with the OxLDL biological activity often varying depending on an LDL donor, the oxidation protocol or endotoxin contamination. Our results agree with earlier studies, which suggest that OxLDL-mediated foam cell formation might not be inflammatory [13]. Further examination of monocyte/macrophage priming by highly purified components of microbial pathogens, DAMPs and their synthetic analogs will bring better clarity to the factors involved in macrophage training in atherosclerosis.

Overall, the data in this study support the hypothesis that persistent inflammarafts serve as effectors of trained immunity in atherosclerosis. The flow cytometry and microscopic methods used in this study may contribute to a toolbox for characterization of macrophage reprogramming in atherosclerosis and identification of new therapeutic targets.

Supplementary Material

Refer to Web version on PubMed Central for supplementary material.

ACKNOWLEDGEMENTS

The authors thank Dr. Nicholas Webster for generously sharing access to a flow cytometer in his lab.

FUNDING

This study was supported by NIH grants HL135737 and HL136275 (to Y.I.M.), NS047101 (to UCSD Microscopy Core), and VA grants I01BX004848 and IBX005224 (to Dr. Nicholas Webster).

REFERENCES

1. Netea MG, Dominguez-Andres J, Barreiro LB, Chavakis T, Divangahi M, Fuchs E, Joosten LAB, van der Meer JWM, Mhlanga MM, Mulder WJM, Riksen NP, Schlitzer A, Schultze JL, Stabell Benn C, Sun JC, Xavier RJ, Latz E. Defining trained immunity and its role in health and disease. Nat Rev Immunol. 2020;20:375–388. [PubMed: 32132681]
2. Flores-Gomez D, Bekkering S, Netea MG, Riksen NP. Trained Immunity in Atherosclerotic Cardiovascular Disease. Arterioscler Thromb Vasc Biol. 2021;41:62–69. [PubMed: 33147995]
3. Kuznetsova T, Prange KHM, Glass CK, de Winther MPJ. Transcriptional and epigenetic regulation of macrophages in atherosclerosis. Nat Rev Cardiol. 2020;17:216–228. [PubMed: 31578516]
4. Miller YI, Navia-Pelaez JM, Corr M, Yaksh TL. Lipid rafts in glial cells: role in neuroinflammation and pain processing. J Lipid Res. 2020;61:655–666. [PubMed: 31862695]
5. Navia-Pelaez JM, Choi SH, Dos Santos Aggum Capettini L, Xia Y, Gonen A, Agatisa-Boyle C, Delay L, Goncalves Dos Santos G, Catroli GF, Kim J, Lu JW, Saylor B, Winkels H, Durant CP, Ghosheh Y, Beaton G, Ley K, Kufareva I, Corr M, Yaksh TL, Miller YI. Normalization of cholesterol metabolism in spinal microglia alleviates neuropathic pain. J Exp Med. 2021;218:e20202059. [PubMed: 33970188]
6. Kim K, Shim D, Lee JS, Zaitsev K, Williams JW, Kim KW, Jang MY, Seok Jang H, Yun TJ, Lee SH, Yoon WK, Prat A, Seidah NG, Choi J, Lee SP, Yoon SH, Nam JW, Seong JK, Oh GT, Randolph GJ, Artyomov MN, Cheong C, Choi JH. Transcriptome Analysis Reveals Nonfoamy Rather Than Foamy Plaque Macrophages Are Proinflammatory in Atherosclerotic Murine Models. Circ Res. 2018;123:1127–1142. [PubMed: 30359200]
7. Tsimikas S, Miyanohara A, Hartvigsen K, Merki E, Shaw PX, Chou MY, Pattison J, Torzewski M, Sollors J, Friedmann T, Lai NC, Hammond HK, Getz GS, Reardon CA, Li AC, Banka CL, Witztum JL. Human oxidation-specific antibodies reduce foam cell formation and atherosclerosis progression. J Am Coll Cardiol. 2011;58:1715–1727. [PubMed: 21982317]
8. Choi SH, Gonen A, Diehl CJ, Kim J, Almazan F, Witztum JL, Miller YI. SYK regulates macrophage MHC-II expression via activation of autophagy in response to oxidized LDL. Autophagy. 2015;11:785–795. [PubMed: 25946330]
9. Fang L, Choi SH, Baek JS, Liu C, Almazan F, Ulrich F, Wiesner P, Taleb A, Deer E, Pattison J, Torres-Vazquez J, Li AC, Miller YI. Control of angiogenesis by AIBP-mediated cholesterol efflux. Nature. 2013;498:118–122. [PubMed: 23719382]
10. Hsieh WY, Zhou QD, York AG, Williams KJ, Scumpia PO, Kronenberger EB, Hoi XP, Su B, Chi X, Bui VL, Khialeeva E, Kaplan A, Son YM, Divakaruni AS, Sun J, Smale ST, Flavell RA, Bensinger SJ. Toll-Like Receptors Induce Signal-Specific Reprogramming of the Macrophage Lipidome. Cell metabolism. 2020;32:128–143 e125. [PubMed: 32516576]
11. Sezgin E, Levental I, Mayor S, Eggeling C. The mystery of membrane organization: composition, regulation and roles of lipid rafts. Nat Rev Mol Cell Biol. 2017;18:361–374. [PubMed: 28356571]
12. Bekkering S, Quintin J, Joosten LAB, Meer JWMvd, Netea MG, Riksen NP. Oxidized Low-Density Lipoprotein Induces Long-Term Proinflammatory Cytokine Production and Foam Cell Formation via Epigenetic Reprogramming of Monocytes. Arterioscler Thromb Vasc Biol. 2014;34:1731–1738. [PubMed: 24903093]

13. Spann NJ, Garmire LX, McDonald JG, Myers DS, Milne SB, Shibata N, Reichart D, Fox JN, Shaked I, Heudobler D, Raetz CR, Wang EW, Kelly SL, Sullards MC, Murphy RC, Merrill AH Jr./ au>, Brown HA, Dennis EA, Li AC, Ley K, Tsimikas S, Fahy E, Subramaniam S, Quehenberger O, Russell DW, Glass CK. Regulated accumulation of desmosterol integrates macrophage lipid metabolism and inflammatory responses. Cell. 2012;151:138–152. [PubMed: 23021221]

HIGHLIGHTS

- Non-foamy macrophages, but not lipid-laden foam cells in mouse atherosclerosis lesions express inflammarafts, enlarged lipid rafts serving as a platform for assembly of inflammatory receptor complexes.
- Inflammarafts are measured by increased levels of lipid rafts and TLR4 dimers and by increased proximity ligation between TLRs, CD36 and lipid rafts, as detected by flow cytometry and imaging.
- Inflammarafts persist in bone marrow-derived macrophages primed with LPS to a hyperinflammatory response to Pam3CSK4.

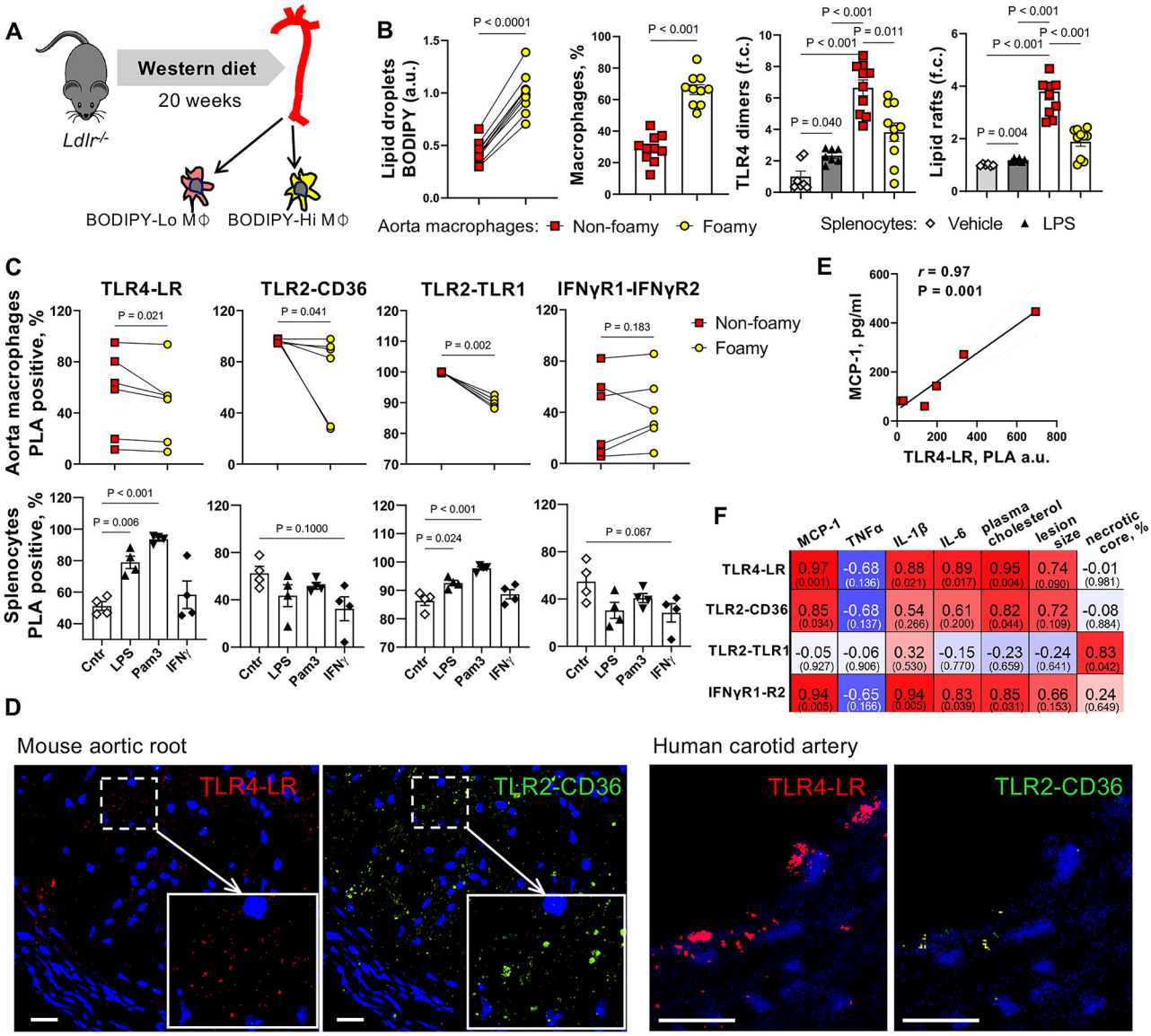

Figure 1. Inflammarafts in non-foamy and foamy macrophages in mouse atherosclerotic lesions.

A, Single-cell suspensions were prepared from whole aorta of *Ldlr*$^{-/-}$ mice (mixed male and female cohort) fed a 0.2% cholesterol, 45% kcal fat diet for 20 weeks, and were gated for BODIPY-hi (foamy) and BODIPY-lo (non-foamy) F4/80 macrophages. **B,** The cells were analyzed for the levels of lipid droplets (Student's pair t-test, n=10), percentage of non-foamy vs. foamy macrophages (Student's t-test, n=10), TLR4 dimers and lipid rafts (one-way ANOVA and Dunnett T3 post-hoc, n=10). **C,** Proximity ligation assay (PLA, n=6) was used to quantify cells expressing TLR4-LR (lipid rafts), TLR2-CD36, TLR2-TLR1, and IFNγR1-IFNγR2 assemblies in aortic foamy vs. non-foamy F4/80 macrophages (Student's paired t-test, n=6) and in splenic F4/80 macrophages stimulated *in vitro* with LPS (100 ng/mL for 15 min), Pam3 (100 ng/mL for 30 min), or IFNγ (50 ng/mL for 30 min) (one-way ANOVA and Tuckey post-hoc, n=4). **D,** Images of PLA detection of TLR4-LR and TLR2-CD36 in sections of mouse aortic root and human endarterectomy specimen. Blue, DAPI. Scale bar, 20 μm. **E-F,** Pearson correlation coefficients and two-tailed P value were

calculated for associations between PLA pairs, plasma levels of MCP-1, TNFα, IL-1β, IL-6 (ELISA), and total cholesterol, aortic root atherosclerotic lesion size (lesion area integrated over 9 sections 100 μm apart), and necrotic core area normalized to lesion size (n=6). Mean±SEM; f.c., fold change; a.u., arbitrary units.

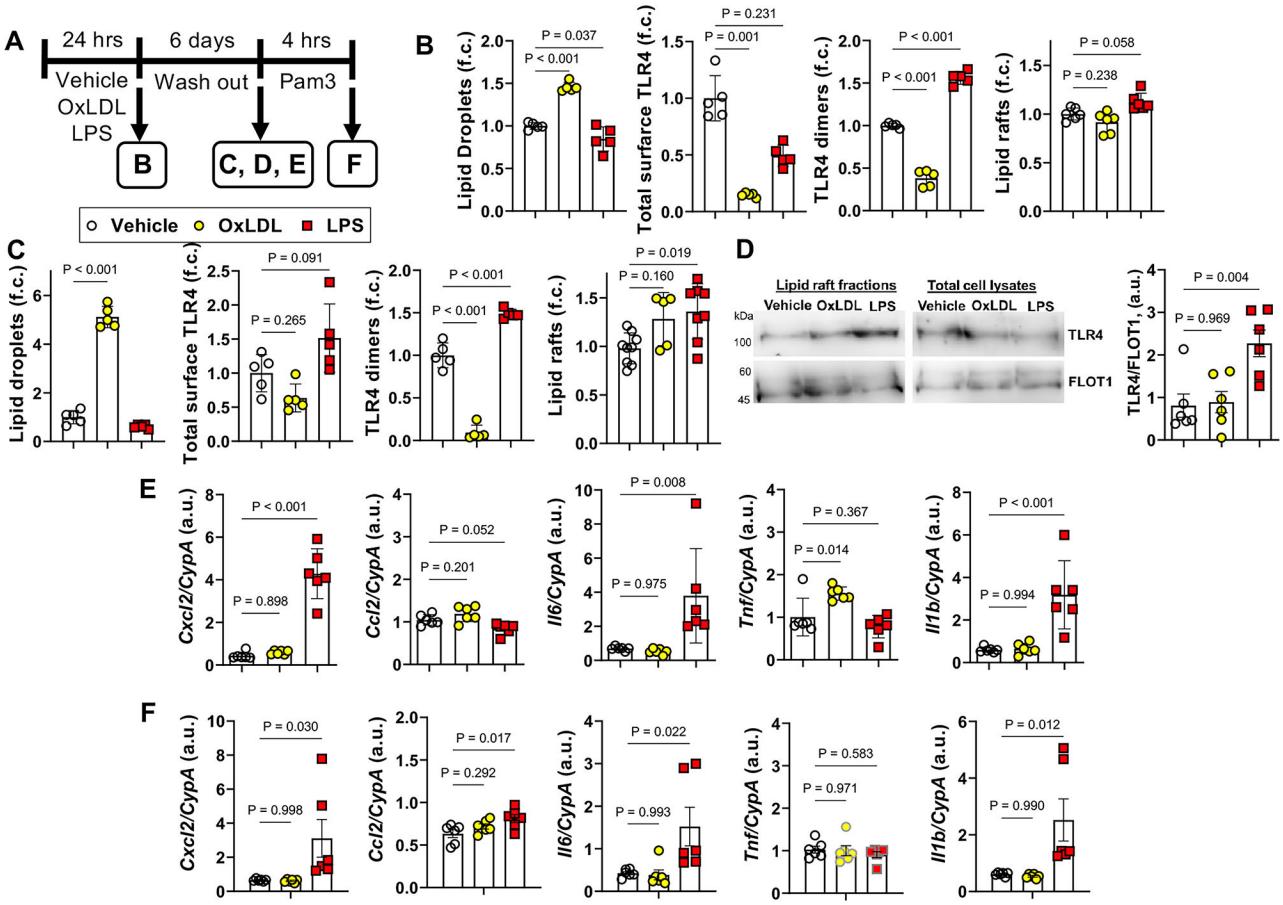

Figure 2. Inflammarafts in macrophages reprogrammed by an exposure to LPS or OxLDL.

A, Experimental design: Murine BMDM were incubated for 24h with LPS (100 ng/mL), OxLDL (20 μg/mL) or vehicle, followed by a 6-day wash-out in the cell culture media without LPS or OxLDL, and then stimulated for 4h by Pam3 (10 ng/ml). The diagram refers to the panels showing the analyses performed at each of these time points. **B and C,** After first 24h stimulation (**B**) and after 6-day wash-out (**C**), cells were analyzed by flow cytometry for lipid droplets (BODIPY), TLR4 expression and dimerization (MTS510 and SA15-21 TLR4 antibodies), and lipid rafts (CTxB). (one-way ANOVA and Tuckey post-hoc, n=5) **D,** After 6-day wash-out, cell lysates were subjected to gradient density ultracentrifugation to isolate lipid raft fractions, which were analyzed by western blot for TLR4 and FLOT1 levels (one-way ANOVA and Tuckey post-hoc, n=6). **E,** After 6-day wash-out, total RNA was isolated to detect mRNA levels of *Cxcl2, Ccl2, Il6, Tnf* and *Il1b*. **E,** Following a 4h Pam3 stimulation (after 6-day wash-out), total RNA was isolated to detect mRNA levels of *Cxcl2, Ccl2, Il6, Tnf* and *Il1b*. For all qPCR results, one-way ANOVA with Tukey's post-hoc test, n=6. Mean±SEM; f.c., fold change; a.u., arbitrary units.